Contact effects in high performance fully printed p-channel organic thin film transistors

Contact effects in high performance fully printed p-channel organic thin film transistors

A. Valletta,[1] A. Daami,[2] M. Benwadih,[2] R. Coppard,[2] G. Fortunato,[1] M. Rapisarda,[1] F. Torricelli,[3] and L. Mariucci[1,a)]
[1]*CNR – IMM, via del fosso del Cavaliere 100, Roma, Italy*
[2]*CEA/LITEN/LCI, 17 rue des martyrs, 38054 Grenoble Cedex 9, France*
[3]*Department of Electrical Engineering, Eindhoven University of Technology, 5600MB Eindhoven, The Netherlands*

(Received 10 October 2011; accepted 19 November 2011; published online 9 December 2011)

Contact effects have been investigated in fully printed p-channel organic thin film transistors with field effect mobility up to 2 cm^2/Vs. Electrical characteristics of the organic thin film transistors, with channel length $<200\,\mu m$, are seriously influenced by contact effects with an anomalous increase of the contact resistance for increasing source-drain voltage. Assuming that contact effects are negligible in long channel transistors and using gradual channel approximation, we evaluated the current-voltage characteristics of the injection contact, showing that I-V characteristics can be modeled as a reverse biased Schottky diode, including barrier lowering induced by the Schottky effect. © *2011 American Institute of Physics*. [doi:10.1063/1.3669701]

The electrical characteristics of organic thin film transistors (OTFTs) are frequently affected by contact effects, which can seriously influence the transistor performance. This is because the "parasitic" voltage drop at the contacts reduces the effective drain-source bias voltage applied to the intrinsic channel of the transistor and, consequently, reduces the device current. Measured contact resistances in OTFTs show a wide range of variation, from few kΩcm up to 10 MΩcm,[1–12] depending upon device configuration, metal contacts,[1–3] and the use of self-assembled monolayers[5,6] to control the metal/organic semiconductor work function difference. In particular, contact resistance appears to be strongly influenced by the device architecture, and much higher values are typically observed in coplanar structures (also known as bottom gate bottom contact) than in staggered structures.[3,4,7,8,12] The importance of the contact resistance is more relevant at large carrier mobility and/or small channel length, where its value may become comparable to, or even larger than, the channel resistance. In general, when scaling the channel length, the condition of comparable on-state channel resistance and contact resistance is encountered at a critical channel length, L_c, and the devices with channel lengths shorter than L_c can be seriously affected by these contact effects, thus preventing the beneficial aspects of device downscaling on the driven current.

In this work, we have studied contact effects in high performance fully printed p-channel OTFTs, to establish the downscaling limitations as well as to characterize and model the contact resistance in such devices.

P-channel OTFTs, with staggered top-gate configuration, were fabricated at CEA-LITEN, using printing processes[13] on heat stabilized, low roughness polyethylene-naphtalate PEN foils (125 μm thick). The source and drain gold contacts were defined by laser ablation (minimum channel length $L = 5\,\mu m$). The p-type semiconductor is a solution processed 6,13-bis(triisopropyl-silylethynyl) pentacene derivative and could be deposited by different techniques such as spin coating or screen printing. The fluoropolymer gate dielectric (1.2 μm thick) and the Ag gate electrode are both deposited by screen printing. All curing steps are kept below 100 °C, to be compatible with the PEN substrate limitation. After its proper annealing, the small-molecules solution-processed semiconductor is observed to form crystallites, which enhances the carrier mobility. The fabricated OTFTs have a multifinger structure with different channel lengths L (from 5 to 200 μm) and channel widths W (from 100 to 2000 μm). From the transfer characteristics measured at low V_{ds} on long channel devices, as shown in Fig. 1, we deduced typical field effect mobility, μ_{FE}, in the range 1.4-2 cm^2/Vs, a threshold voltage, V_T, between −10 V and −15 V and a subthreshold swing, S, of 5-7 V/dec. Field effect mobility evaluated from saturated transfer characteristics, μ_{sat}, is in the range 0.9–1.4 cm^2/Vs. The output characteristics, reported in Fig. 2, show linear behavior at low $|V_{ds}|$, suggesting a low contact resistance, in agreement to what has been already observed in staggered OTFTs.[4] In order to test if the electrical characteristics follow the conventional square-law equation, we have plotted in Fig. 1 the normalized drain current, I_d/V_{ds}, vs V_g-$V_{ds}/2$ for transistors with different channel lengths. In the case of a long channel ($L = 200\,\mu m$) device, the normalized transfer characteristics measured at different V_{ds} are perfectly superposed (see Fig. 1 panel (a)), confirming that the electrical characteristics follow the square-law theory. On the other hand, scaling down the transistor channel length (i.e., $L = 10\,\mu m$), the normalized drain current shows substantial departure from the expected behavior. We have also tested the applicability of gradual channel approximation (GCA) by comparing the measured output characteristics of devices with different channel lengths, with the following equation:

$$I_d = \frac{W}{L}\int_{V_{gs}-V_{ds}}^{V_{gs}} G(V)dV, \qquad (1)$$

a)Author to whom correspondence should be addressed. Electronic mail: luigi.mariucci@cnr.it.

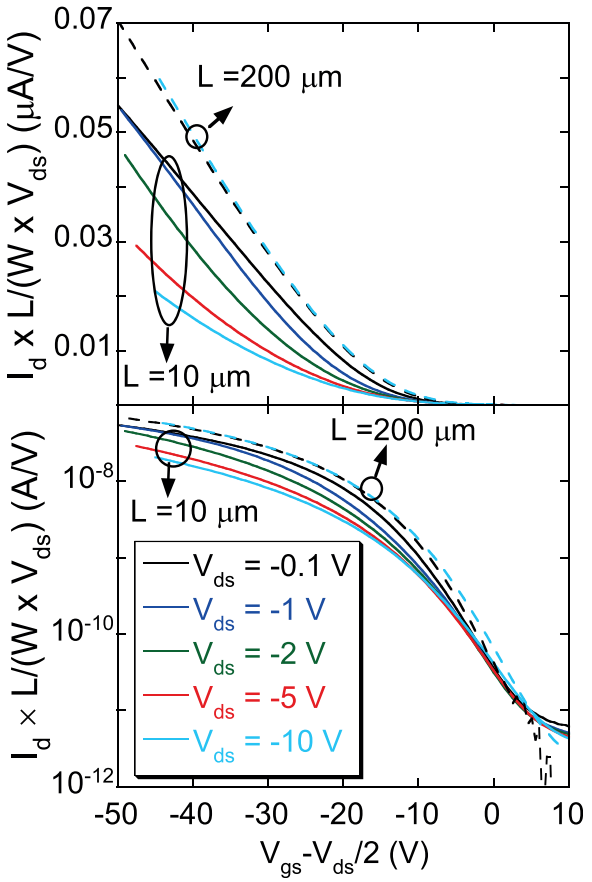

FIG. 1. (Color online) Normalized transfer characteristics of long (L = 200 μm, dashed lines) and short (L = 10 μm, solid lines) channel OTFTs measured at different drain voltages.

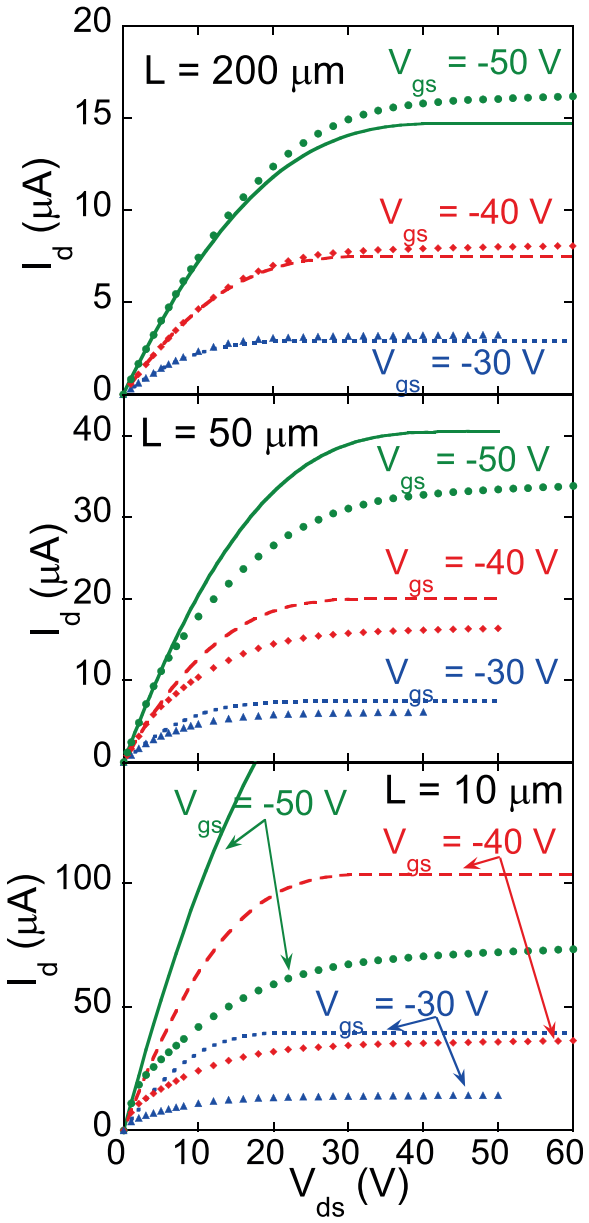

FIG. 2. (Color online) Experimental output characteristics (symbols), measured at different gate voltages, of OTFTs with three different channel lengths. Lines show the theoretical output characteristics calculated by using the gradual channel approximation.

where $G(V) = I_d(V_{gs})/V_{ds}$ is the channel conductance determined by the transfer characteristics measured at low V_{ds} (0.1 V). As it can be seen from Fig. 2, GCA theory reproduces the output characteristics only in the case of long channel devices. Nevertheless, as the channel length is scaled down, GCA progressively fails in reproducing the experimental $I_d(V_{ds})$ curves, predicting much higher saturation currents. These data clearly suggest the presence of contact effects, which become progressively evident as the channel length is scaled down and as V_{ds} increases.

The observed increase of the contact effects with V_{ds} is rather anomalous, if compared with previous observations. In fact, in the case of coplanar structures, the contact effects are more pronounced at low V_{ds}, resulting in superlinear I_d-V_{ds} characteristics at low V_{ds}.[2,4–6] In this case, the contact current shows an exponential increase as a function of the potential drop, V_c, over the contact region.[4,6] As a consequence of this, the contact resistance substantially decreases for increasing V_{ds}, often becoming negligible in the saturation regime.[6] For this reason, field effect mobility values in coplanar devices are often extracted from saturated characteristics, as those deduced from the linear regime are much lower and strongly affected by the parasitic resistance effects. In contrast, in our short channel devices, we observed exactly the opposite: the field effect mobility extracted from saturated characteristics is much lower than the one determined from the linear regime (low-V_{ds}). In the case of staggered OTFTs, contact resistance appears to be constant with V_{ds} (ohmic contacts), as determined by the gated four point probe measurements[9] or by measurements on devices with different channel length, L,[3] and to decrease with increasing V_g.[3,9,10] The gate bias dependence has been explained by considering the current crowding effect, which results in an increased contact area as the channel gets more and more accumulated[9,10] and space charge limited current in the bulk of the organic active layer.[10] An alternative approach to explain the gate bias dependence of the contact resistance in polycrystalline organic semiconductors based TFTs has been proposed by Vinciguerra *et al.*,[11] who considered a combination of grain boundary trapping model, including an exponential density of trap states localized at the grain boundaries (Meyer-Neldel model[14]) and Schottky contacts.

In order to evaluate the contact current-voltage characteristics in our devices, we adopted a common approach,[4,6]

splitting the channel into a small contact region at the source electrode, where there is a voltage drop V_C, and the main channel where the voltage drop is V_{DS}–V_C. As already shown in Figs. 1 and 2, long channel devices follow closely the GCA, denoting negligible contact effects (channel resistance ≫ contact resistance). Hence, we evaluated the channel conductance G(V) from the long channel transfer characteristics and we determined the contact potential drop, V_C, by solving the following equation in the case of short channel devices and for a given set of I_d, V_{gs}, and V_{ds}:

$$I_d = \frac{W}{L}\int_{V_{gs}-V_{ds}}^{V_{gs}-V_c} G(V)dV. \quad (2)$$

The resulting I_d-V_C curves deduced for different V_{gs} and reported in Fig. 3 closely resemble the characteristics of a reverse biased leaky diode. Therefore, we have fitted the I_d-V_c curves with the following Schottky diode relationship:

$$I_d = -I_0 \exp\left[\left(\frac{V_c}{V_0}\right)^{\alpha}\right]\left\{\exp\left[-\left(\frac{qV_c}{\eta kT}\right)\right]-1\right\}, \quad (3)$$

where I_0 is the reverse current for $V_{ds} = 0$ V, the second term takes into account the barrier lowering induced by the Schottky effect, which depends on the electric field at the junction, E, which itself depends upon V_C, with V_0 and α as fitting parameters. The third term is the classical diode relationship, with η being the quality factor. It should be pointed out that the Schottky effect has been directly observed in metal/polymer interface by using internal photoemission spectroscopy.[15] A very good reproduction of the I_d-V_C curves is achieved with the following values of the fitting parameters: $V_0 = 0.34$ V, $\alpha = 0.25$ (see Fig. 3). We note that in inorganic semiconductors, the electric field at the Schottky junction is expected to be proportional to $(V_{bi}\text{-}V)^{1/2}$, where V_{bi} is the built-in potential, and that the Schottky effect induces a barrier height reduction $\Delta\Phi = (qE/4\pi\varepsilon_s)^{1/2}$ (where ε_s is the semiconductor permittivity),[16] thus leading to $\Delta\Phi$ proportional to $V^{1/4}$, which is in good agreement with our fitting α-value. The diode reverse current I_0 is actually found to depend on the gate bias. A plot of such dependence for the three short channel devices is reported in the inset of Fig. 3.

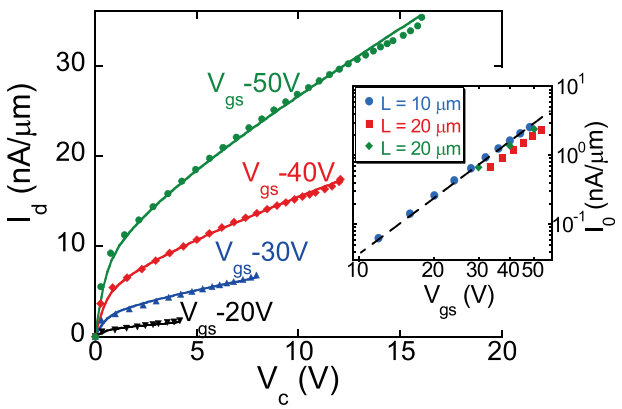

FIG. 3. (Color online) Current voltage characteristics of the source contact, evaluated for different gate voltages, of an OTFT with L = 10 μm (symbols) and corresponding fits calculated by using Eq. (3) (lines). Inset shows the diode reverse current, I_0, as a function of gate voltages for devices with different L.

The three curves follow very closely the same trend and I_o can be approximated, in the V_{gs} range considered, as a power law

$$I_0 = I_{00}\left(\frac{V_{gs}}{V_{00}}\right)^{\beta}, \quad (4)$$

where the constant $I_{00} = 8\times10^{-14}$ A/μm and the exponent $\beta = 2.7$, as extracted from best fitting of the experimental data, while V_{00} has been introduced to keep the dimensionality of the pre-factor I_{00} (V_{00}-value has been arbitrary set to 1). The dependence of I_0 from V_g could be explained by noting that the source contact is acting as a gated Schottky diode. Indeed, as already suggested by Vinciguerra *et al.*,[11] a contribution to the gate bias dependence of the contact resistance, R_s, arises from the gate modulation of the Schottky barrier at the source/drain contacts. Consequently, as can be seen in Fig. 4(a), contact resistance decreases with increasing V_{gs} for fixed V_{ds}, whereas for a given V_{gs}, R_s increases with increasing V_{ds} as the voltage drop V_c at the contact increases. Furthermore, Fig. 4(a) shows that, for L = 10 μm, R_s is comparable or higher than channel resistance even for

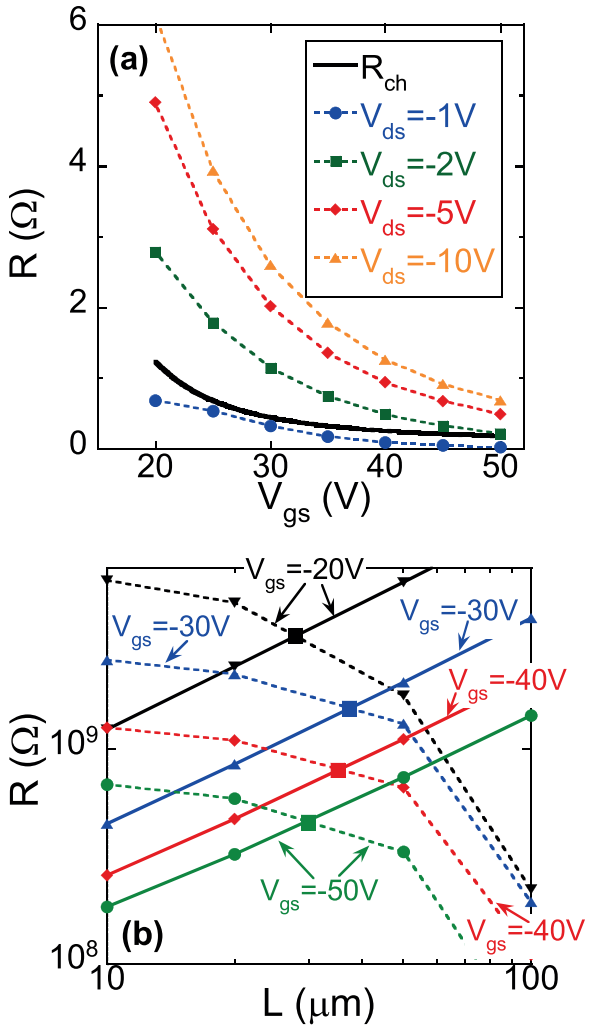

FIG. 4. (Color online) (a) Contact resistance, R_s (dashed lines), evaluated at different V_{ds}, and channel resistance, R_{ch} (solid line), vs gate voltage of an OTFTs with L = 10 μm. (b) Contact resistance (dashed lines) and channel resistance (solid lines), calculated for a fixed V_{ds} (−10 V) and different V_{gs}, as a function of L.

V_{ds} as low as -1 V, then contact resistance becomes dominant in the electrical characteristics of short channel OTFTs. For increasing channel length, R_s decreases (Fig. 4(b)) showing a similar behavior for all V_{gs}. This R_s reduction can be related to the different V_{ds} partition between the contact and the channel resistances. Indeed, for a given value of V_{ds}, by increasing L, R_{ch} linearly increases, inducing a larger voltage drop, V_d-V_c, on R_{ch}, thus reducing the voltage drop, V_c-V_s, on R_s. As a result, considering the I_d-V_c curves shown in Fig. 3, a lower differential resistance of the diode at the source contact is expected. Fig. 4(b) also shows that, for the bias condition considered, R_s and R_{ch} become comparable for OTFTs with L between 30 and 40 μm suggesting that the critical L_c value should be placed in this range.

According to the presented analysis, we have then implemented an equivalent circuit of the OTFTs, consisting of a reverse biased diode in series with an "ideal" transistor, i.e., a transistor following GCA and whose G(V) is extracted from the long channel characteristics. The compact model allows to perfectly reproduce the electrical characteristics of devices with different geometries and it has been implemented in a computer-aided design (CAD) system in order to perform circuit simulations.

In conclusion, contact effects have been investigated in fully printed p-channel organic thin film transistors with field effect mobility up to 2 cm^2/Vs. Contact effects seriously influence the electrical characteristics in devices with channel length $<200\,\mu$m and we found a drastic increase of the contact resistance for increasing source/drain voltage. Assuming that contact effects are negligible in long channel devices, as confirmed by the applicability of the gradual channel approximation, we developed a method to extract the current-voltage characteristics of the source contact. The I-V contact characteristics were modeled as a reverse biased Schottky diode, including barrier lowering induced by this Schottky effect and gate modulation of the reverse current. The developed compact model allows a nice reproducibility of the device characteristics for different geometries and has been applied to circuit simulations.

This work has been funded in the frame of the European FP7 project COSMIC (Grant Agreement No. 247681)

[1]D. J. Gundlach, L. Zhou, J. A. Nichols, T. N. Jackson, P. V. Necliudovc, and M. S. Shur, J. Appl. Phys. **100**, 024509 (2006).
[2]B. H. Hamadani and D. Natelson, J. Appl. Phys. **97**, 064508 (2005).
[3]P. V. Necliudov, M. S. Shur, D. J. Gundlach, and T. N. Jackson, J. Appl. Phys. **88**, 6594 (2000).
[4]R. A. Street and A. Salleo, Appl. Phys. Lett. **81**, 2887 (2002).
[5]N. Kawasaki, Y. Ohta, Y. Kubozono, and A. Fujiwara, Appl. Phys. Lett. **91**, 123518 (2007).
[6]Y. Hong, F. Yan, P. Migliorato, S. H. Han, and J. Jang, Thin Solid Films **515**, 4032 (2007).
[7]I. G. Hill, Appl. Phys. Lett. **87**, 163505 (2005).
[8]Y. Xu, T. Minari, K. Tsukagoshi, J. A. Chroboczek, and G. Ghibaudo, J. Appl. Phys. **107**, 114507 (2010).
[9]T. J. Richards and H. Sirringhaus, J. Appl. Phys. **102**, 094510 (2007).
[10]S. D. Wang, Y. Yan, and K. Tsukagoshi, Appl. Phys. Lett. **97**, 063307 (2010).
[11]V. Vinciguerra, M. La Rosa, D. Nicolosi, G. Sicurella, and L. Occhipinti, Org. Electron. **10**, 1074 (2009).
[12]L. Mariucci, D. Simeone, S. Cipolloni, L. Maiolo, A. Pecora, G. Fortunato, and S. Brotherton, Solid State Electron. **52**, 412 (2008).
[13]A. Daami, C. Bory, M. Benwadih, S. Jacob, R. Gwoziecki, I. Chartier, R. Coppard, C. Serbutoviez, L. Maddiona, E. Fontana, and A. Scuderi., in *ISSCC Dig. Tech. Papers* (IEEE-SSCS. Piscataway, USA, 2011), pp. 328–330.
[14]W. Meyer and H. Neldel, Z. Tech. Phys. (Leipzig) **18** (1937) 588.
[15]G. L. J. A. Rikken, D. Braun, E. G. J. Staring, and R. Demandt, Appl. Phys. Lett. **65**, 219 (1994)
[16]S. M. Sze, *Physics of Semiconductor Devices* (Wiley, New York, 1981), p. 257.